BRIEF REPORT

Setting constrains on the $WW\gamma\gamma$ Vector Boson Coupling

Claire Yang (ID: 260898597)

Supervised by Brigitte Vachon, John McGowan and Xingguo Li.
This manuscript was compiled on June 30, 2024

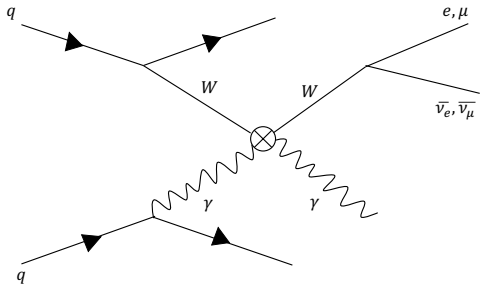

Fig. 1. Feynman diagram of the $WW\gamma\gamma$ vertex (5).
q stands for quark, W for W boson, γ for photon, e, μ are the leptons, $\bar{\nu}$ for neutrino. The quarks and photons emitted cannot be observed directly, so instead, they are treated as a jet of particles

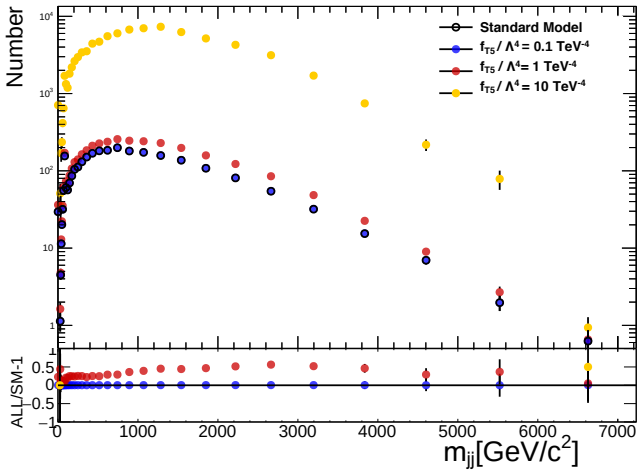

Fig. 2. The raw truth data of the kinematic variable m_{jj}. The three coupling values of $f_{T5}/\Lambda^4 = \{0, 1, 1, 10TeV^{-4}\}$ were superimposed to see the deviations between the standard model expectation and with the presence of the operator $\mathcal{O}_{T,5}$. The histogram of the Standard Model is not noticeable on the graph due to its close proximity to the histogram of the first coupling value.

Studies of the deviation between the performance of gauge bosons in the proton-proton collision and the predictions of the Standard Model may guide us to new physics. This deviation can be quantified by the effective field theory which builds a Lagrangian function beyond the Standard Model(1). This function has a set of unknown parameters representing the strength of the boson coupling. In this study, we mainly focused on the $WW\gamma\gamma$ coupling and analyzed it with a software tool, which uses the maximum likelihood estimation method(2) to estimate the confidence interval of the coupling strength. We tested its robustness after applying modifications to it. The results indicate that the confidence interval of our parameters is correctly widened as the systematic uncertainties grow. The fit results using the Asimov data set(3) are all centered on point 0. This demonstrates the feasibility of this software tool. The results tell us that the T-type operator(4), especially $\mathcal{O}_{T6}$, $\mathcal{O}_{T1}$, and $\mathcal{O}_{T5}$, is particularly sensitive to the $WW\gamma\gamma$ coupling compared to the M-type operator.

The interactions between gauge bosons (W, Z, and photon) in proton-proton collisions are specified in the Standard Model of Particle Physics. Deviations from predictions would give a hint to new physics phenomena. The coupling of electroweak gauge bosons beyond the Standard Model is one of the processes indicating new physics phenomena, also referred to as Vector boson scattering (VBS). As described in the Standard Model, the rate of reaction in the proton-proton collision is dependent to the strength of interaction of the gauge bosons. Thus one of the possible electroweak boson coupling, namely $WW\gamma\gamma$ coupling, as in Fig.1 is of our interest.

Acquiring more knowledge about the coupling involves setting constraints on it. To achieve this, we studied a software tool and contributed to its development, and investigated the impact of systematic uncertainties on the resulting data within this tool.

We presented data on the kinematic variables called the invariant mass of jets m_{jj} of the above coupling, with the existence of certain operators which will be introduced in next section. The plot in fig.2 from the previous study provides some idea of what the raw data looks like. It shows the distribution of events as a function of m_{jj}.

Materials and Methods

Theory. Effective field theory (EFT) (1) is a powerful tool to build new physics beyond a particular model. It is model-independent, thus nicely suited for our computation of boson coupling beyond the Standard Model. Here we aim to derive the Lagrangian function of SMEFT, the so-called Effective field theory of the Standard Model. This function allows us to add impacts of several operators to the prediction of the Standard Model:

$$\mathcal{L}_{EFT} = \mathcal{L}_{SM} + \sum_{n\geq 5}\sum_{i}\frac{c_i}{\Lambda^{n-4}}\mathcal{O}_i^{(n)} \qquad [1]$$

where n represents the dimension. c_i is the coefficient to the operators, also known as coupling values, which is unknown to people so far. Λ is the energy scale and $\mathcal{O}_i$ is the operator describing the new physics interaction. According to a study (4) at LHC, the operators contributing to the $WW\gamma\gamma$ coupling are namely: {M0, M1, M2, M3, M4, M5, M7, T0, T1, T2, T5, T6, T7}. Note that in the proton-proton collision, there are three types of operators representing by characters S, T, and M respectively. The S stands for scale (longitudinal) operator, T stands for transverse operator, and M for mixed transverse and longitudinal operator. The numbers after are simply for numbering.(6)

The estimation of the unknown parameters c_i corresponding to the above set of operators is of interest to us. This can be achieved through the maximum likelihood estimation (MLE) method(2). For a given dataset $\boldsymbol{x} = (x_1, x_2, ...x_n)$ of n measurements in total, the probability density function is defined to be $f(x_i; \boldsymbol{\theta})$, where $\boldsymbol{\theta} = (\theta_1, \theta_2, ...\theta_m)$ is the set of parameters of interest. In this case, the likelihood function is:

$$L(\boldsymbol{x}; \boldsymbol{\theta}) = \prod_{N}^{i=1} f(x_i; \boldsymbol{\theta}). \quad [2]$$

Hence one can obtain the estimate value $\hat{\boldsymbol{\theta}}$ by finding which brings $L(\boldsymbol{x}; \hat{\boldsymbol{\theta}})$ to the global maximum.

If we manipulate this equation in logarithmic form, the so-called log-likelihood function, it would be simpler to carry out. At this point, obtaining the estimated value turns into the search for the global minimum of this function:

$$-\ln L(\boldsymbol{x}; \boldsymbol{\theta}) = -\sum_{i=1}^{n} \ln f(x_i; \boldsymbol{\theta}). \quad [3]$$

The best estimator of parameters only cares about the extreme value of the above function. On the other hand, the shape of the function is also worthwhile, as it can be used to predict the uncertainty, or rather to calculate the confidence interval. This brings in the helpfulness of the log-likelihood function, in which we apply a χ^2 test on the likelihood function to see the confidence interval of the parameters c_i. The 95% confidence interval is evaluated by the integral of the χ^2 function (7):

$$95\% < \int_0^{q(c_X)} \chi^2(degree\ of\ freedom = 1)dq, \quad [4]$$

where $q(c_X)$ is the profile likelihood ratio test statistic. The χ^2 function is:

$$\chi^2(c_X, \boldsymbol{\theta}) = \boldsymbol{\sigma}^T C^{-1} \boldsymbol{\sigma}, \quad [5]$$

and

$$\boldsymbol{\sigma} = (\boldsymbol{\sigma}_{data} - \boldsymbol{\sigma}_{theory} - \sum_{\theta} \theta \boldsymbol{e}_\theta). \quad [6]$$

where $\boldsymbol{\sigma}_{data}$ is the cross-section of data, $\boldsymbol{\sigma}_{theory}$ is the theory predicted cross-section for c_X, C is the sum of the statistical and systematic covariance matrices on $\boldsymbol{\sigma}_{data}$ data. $\boldsymbol{\theta}$ is the vector of nuisance parameters, where each component θ is corresponding to a truth-level uncertainty on Standard Model prediction, with an absolute magnitude equal to $\boldsymbol{e}_\theta$.

Data. To check the validity of the analysis tool before the blind analysis with the actual experimental data, we used the Asimov data set(3) for fitting. It is the simulated data to a average sensitivity for multidimensional parameter space beyond the Standard Model. Thus any new physics phenomena are not expected to present with this data set. In other words, the best-fit result of the parameters $\boldsymbol{\theta}$ is expected to be centered at 0.

The data set we used is already available before. They are generated using the `MADGRAPH` framework, which is based on the Monte Carlo generator(8). The measurement data is separated into three parts:

$$|\mathcal{M}|^2 = |\mathcal{M}_{SM}|^2 + 2Re(\mathcal{M}^*_{SM}\mathcal{M}_{\mathcal{O}_i}) + \mathcal{O}_i(\Lambda^{-4}). \quad [7]$$

the best Standard Model prediction($|\mathcal{M}_{SM}|^2$), the linear effects that contribute by the interference of the predicted coupling and the operators $2Re(\mathcal{M}_{SM}\mathcal{M}_{\mathcal{O}_i})$, the quadratic effect that contributes by the operators $\mathcal{O}_i(\Lambda^{-4})$. All data used in this report includes all three parts above.

Technical approach. The maximum likelihood estimation on parameters is implemented by a common software tool developed by ATLAS collaborators. After understanding its structure, some adjustments were made to verify its performance under various systematic uncertainties.

When analyzing a specific parameter c_j for operator $\mathcal{O}_j$, computation on only one-dimensional limits is required. This can be achieved by treating all other parameters c_i's as nuisance parameters and setting them as constant in the likelihood function. With such a setup, we simulated several sources of uncertainties. The data set and these simulated uncertainties are fed to the software tool through a configuration file, so that we can generate a model based on these inputs. With this model, we scanned over a range of possible values for the parameterc_i with the software, and calculates the log-likelihood function for these values. This yields a plot with a log-likelihood function over c_i. As introduced in the Theory section, the global minimum of this plot is the best estimator, which is expected to have the log-likelihood function approaching 0. The 95% and one standard deviation (i.e. 68%) interval can be obtained with Eqn.4. Therefore, by modifying the configuration files and doing the scan with it, we are able to visualize and quantify the variations in the performance under different systematic uncertainties. According to the variations, we can confirm the reliability of this tool regarding the uncertainty processing.

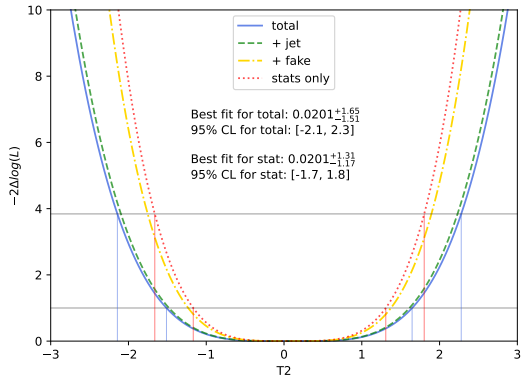

Fig. 3. Scan over a range of the coupling value of $\mathcal{O}_{T2}$ to do the log-likelihood fitting with or without four sources of systematic uncertainties. The upper horizontal line stands for the 68% confidence interval (one standard deviation) and the lower horizontal line stands for 95%.

Result

For the set of operators that contribute to the $WW\gamma\gamma$ coupling, we simulated different sources of the measurement uncertainties to see the impact they bring to the confidence interval as mentioned in the last section. There are mainly four sources of uncertainties for simulation, namely statistical uncertainties, fake, jet energy, and other uncertainties. Fig. 3 takes the operator $\mathcal{O}_{T2}$ as an example to show the effects of the uncertainties. The narrowest curve arises when there are the least sources of uncertainties, i.e. when there are only statistical uncertainties. On this basis we included the fake uncertainty, making the shape a little wider. Then we put in the uncertainties brought by the jet energy, and it is noticeable that the shape extended significantly. Lastly, the other minor uncertainties were added, meaning the curve includes full uncertainties. It seems to be close to the previous curve, indicating that the contribution of the other uncertainties is not very significant.

According to Eqn.6, adding systematic uncertainties increasing $\boldsymbol{e}_\theta$, thus smaller $\boldsymbol{\sigma}$, which require higher $q(c_X)$ to reach a certain percentage. So we expect a broader range of the confidence level of the parameters of interest with more uncertainties joined in. In fact, each entry of the uncertainty source broadens the confidence interval of the function as in Eqn.4, which is consistent with the expectation. The best-fit and confidence interval results with all four systematic uncertainties and with only the statistical uncertainties are printed in the diagram, which also enabled us to reconfirm the effect of uncertainties on the widening of the confidence interval range numerically.

All the other operators we are working with are indicating the same conclusion as the T2 operator. The table 1 below summarized the best-fit and 95% confidence interval results, both with the statistical uncertainty only and with full uncertainties. The uncertainty range in the columns of best-fit result is one standard deviation, i.e. the 68% confidence interval. For all the operators, the best fit result is considered reasonable, given that 0 is always within one standard deviation. This confirms the accuracy of this software tool's estimation of best fit result, within the Asimov data set.

By analyzing the data in the table, we can derive the following digitized information:

- Comparing the consequences of systemic uncertainties, the 95% and 68% confidence intervals in the table show that the results with full uncertainty are about 20% to 30% larger than those with statistical uncertainty only, for both T-type and M-type operators.
- For the averaged value, the confidence interval of T-type operators is approximately 13 times tighter than that of M-type. This indicates that the Asimov data set expects T-type operators to be more sensitive to the $WW\gamma\gamma$ coupling than M-type under the same conditions.
- The most restricted interval appears with operator $\mathcal{O}_{T6}, \mathcal{O}_{T1}, \mathcal{O}_{T5}$. These three operators are considered to be most sensitive to the coupling under the expectation of the Asimov data set.

The above results all agree that this software tool is robust, probably a data set other than Asimov can be used to feed it in the future.

Conclusion

To summarize, in an attempt to set constraints on $WW\gamma\gamma$ vertex to determine the strength of the coupling, we learned about the software tool provided by the ATLAS collaborators. We modified it and used it to construct the constraint interval. In the experiment, we confirmed the accuracy and reliability of the software. It properly reflected the widening of the confidence interval for larger systematic errors. Additionally, it accurately estimated the fit value of each constraint for the Asimov data set. Besides, our result data implies that the T-type operators are more sensitive to $WW\gamma\gamma$ coupling than M-type, especially $\mathcal{O}_{T6}$, $\mathcal{O}_{T1}$, and $\mathcal{O}_{T5}$ operators.

Acknowledgements

Gratitude goes to Prof. Brigitte Vachon and the ATLAS $W\gamma\gamma$ group. Special thanks to Prof. Brigitte Vachon for theoretical guidance, John McGowan for providing simulated data and operational guidance, and the ATLAS collaborators for supplying the code framework.

References

1. B Grzadkowski, M Iskrzyński, M Misiak, J Rosiek, Dimension-six terms in the standard model lagrangian. *J. High Energy Phys.* **2010** (2010).
2. O Behnke, L Moneta, *Parameter Estimation.* (John Wiley & Sons, Ltd), pp. 27–73 (2013).

Table 1

Operator	Best fit with stats only	95% interval with stats only	Best fit with full uncertainty	95% interval with full uncertainty
M0	$-0.2^{+8.7}_{-8.5}$	[-12., 12.]	$0.0^{+10.6}_{-10.8}$	[-15., 15.]
M1	$0.0^{+13.0}_{-12.6}$	[-18., 18.]	$0.0^{+15.8}_{-16.2}$	[-22., 23.]
M2	$0.0^{+3.1}_{-3.1}$	[-4.4, 4.3]	$0.0^{+3.8}_{-3.9}$	[-5.4, 5.4]
M3	$0.0^{+4.5}_{-4.6}$	[-6.3, 6.4]	$0.0^{+5.6}_{-5.6}$	[-7.8, 7.9]
M4	$0.0^{+5.4}_{-5.5}$	[-7.6, 7.6]	$0.0^{+6.7}_{-6.8}$	[-9.5, 9.5]
M5	$0.0^{+5.0}_{-4.0}$	[-5.8, 6.9]	$0.0^{+6.6}_{-4.8}$	[-7.1, 8.8]
M7	$-0.4^{+22.8}_{-22.6}$	[-32., 32.]	$0.0^{+28.5}_{-28.2}$	[-40., 40.]
T0	$0.0^{+0.7}_{-0.6}$	[-.90, .92]	$0.0^{+0.8}_{-0.8}$	[-1.1, 1.2]
T1	$0.0^{+0.4}_{-0.4}$	[-.58, .61]	$0.0^{+0.5}_{-0.5}$	[-.74, .77]
T2	$0.0^{+1.3}_{-1.2}$	[-1.7, 1.8]	$0.0^{+1.6}_{-1.5}$	[-2.1, 2.3]
T5	$0.0^{+0.4}_{-0.5}$	[-.64, .64]	$0.0^{+0.6}_{-0.6}$	[-.81, .82]
T6	$0.0^{+0.4}_{-0.4}$	[-.52, .53]	$0.0^{+0.5}_{-0.5}$	[-.66, .67]
T7	$0.0^{+1.0}_{-1.0}$	[-1.4, 1.4]	$0.0^{+1.3}_{-1.3}$	[-1.8, 1.8]

3. G Cowan, K Cranmer, E Gross, O Vitells, Asymptotic formulae for likelihood-based tests of new physics. *The Eur. Phys. J. C* **71** (2011).
4. D Green, P Meade, MA Pleier, Multiboson interactions at the LHC. *Rev. Mod. Phys.* **89** (2017).
5. R Gomez-Ambrosio, Vector Boson Scattering Studies in CMS: The $pp \to ZZjj$ Channel. *Acta Phys. Pol. B Proc. Suppl.* **11**, 239–248. 10 p (2018).
6. Limits on anomalous triple and quartic gauge couplings (2020).
7. G Aad, et al., Measurements of differential cross-sections in four-lepton events in 13 tev proton-proton collisions with the atlas detector. *J. High Energy Phys.* **2021**, 5 (2021).
8. J Alwall, M Herquet, F Maltoni, O Mattelaer, T Stelzer, MadGraph 5: going beyond. *J. High Energy Phys.* **2011** (2011).